Evolution from BCS to BEC Superfluidity in *p*-Wave Fermi Gases

M. Iskin and C. A. R. Sá de Melo
School of Physics, Georgia Institute of Technology, Atlanta, Georgia 30332, USA
(Received 11 October 2005; published 31 January 2006)

We consider the evolution of superfluid properties of a three-dimensional p-wave Fermi gas from a weak coupling Bardeen-Cooper-Schrieffer (BCS) to strong coupling Bose-Einstein condensation (BEC) limit as a function of scattering volume. At zero temperature, we show that a quantum phase transition occurs for p-wave systems, unlike the s-wave case where the BCS to BEC evolution is just a crossover. Near the critical temperature, we derive a time-dependent Ginzburg-Landau (GL) theory and show that the GL coherence length is generally anisotropic due to the p-wave nature of the order parameter, and becomes isotropic only in the BEC limit.

DOI: 10.1103/PhysRevLett.96.040402 PACS numbers: 03.75.Ss, 03.75.Hh, 05.30.Fk

Arguably the next frontier of research in ultracold Fermi systems is the search for superfluidity in higher angular momentum states. Substantial experimental progress has been made recently [1–5] in connection to p-wave cold Fermi gases, making them ideal candidates for the observation of novel triplet superfluid phases. These phases may be present not only in atomic but also in nuclear (pairing in nuclei), astrophysics (neutron stars), and condensed matter (organic superconductors) systems.

The tuning of p-wave interactions in ultracold Fermi gases was initially explored via p-wave Feshbach resonances in trap geometries for ^{40}K [1,2] and ^{6}Li [3,4]. Finding and sweeping through these resonances is difficult since they are much narrower than the s-wave ($\ell = 0$) case, because atoms interacting via higher angular momentum channels ($\ell \neq 0$) have to tunnel through a centrifugal barrier to couple to the bound state [2]. Furthermore, while losses due to two-body dipolar [3,6] or three-body [1,2] processes challenged earlier p-wave experiments, these losses were still present but were less dramatic in the very recent optical lattice experiment involving ^{40}K and p-wave Feshbach resonances [5].

For a dilute ^{40}K Fermi gas, the magnetic dipole-dipole interactions between valence electrons split p-wave ($\ell = 1$) Feshbach resonances that belong to different m_ℓ states [2]. Therefore, the ground state is highly dependent on the detuning and separation of these resonances, and possible p-wave superfluid phases can be studied from the Bardeen-Cooper-Schrieffer (BCS) to the Bose-Einstein condensation (BEC) regime. For instance, it has been proposed [7,8] for sufficiently large splittings that pairing occurs only in $m_\ell = 0$ and does not occur in the $m_\ell = \pm 1$ state, while for small splittings, pairing occurs via a linear combination of the $m_\ell = 0$ and $m_\ell = \pm 1$ states. Thus, these resonances may be tuned and studied independently if the splitting is large enough in comparison to the experimental resolution.

The BCS to BEC evolution in p-wave systems was recently discussed at $T = 0$ for a two-hyperfine state (THS) [9] in three dimensions (3D), and for a single-hyperfine state (SHS) [10,11] in two dimensions, using fermion-only models. Furthermore, fermion-boson models were proposed to describe p-wave superfluidity at zero [7,8] and finite temperature [12] in three dimensions. Unlike the previous models, we present a zero and finite temperature analysis of a SHS Fermi gas in 3D within a fermion-only description, where molecules naturally appear as bound states of two-fermions. The main results of our Letter are as follows: (a) the BCS to BEC evolution in p-wave systems requires a new length scale in addition to the scattering volume, while in s-wave systems only the scattering length is sufficient; (b) a quantum phase transition occurs as a function of scattering volume in contrast with the s-wave case, where the BCS to BEC evolution is a crossover; (c) the time-dependent Ginzburg-Landau (TDGL) theory has anisotropic coherence lengths which become isotropic only in the BEC limit, in sharp contrast to the s-wave case, where the coherence length is isotropic for all couplings.

We start with the Hamiltonian ($\hbar = 1$)

$$H = \sum_{\mathbf{k}} \xi(\mathbf{k}) a^\dagger_{\mathbf{k},\uparrow} a_{\mathbf{k},\uparrow} + \frac{1}{2} \sum_{\mathbf{k},\mathbf{k}',\mathbf{q}} V_p(\mathbf{k},\mathbf{k}') b^\dagger_{\mathbf{k},\mathbf{q}} b_{\mathbf{k}',\mathbf{q}}, \quad (1)$$

for a dilute SHS p-wave Fermi gas in 3D, where the pseudospin $\uparrow$ labels the hyperfine state represented by the creation operator $a^\dagger_{\mathbf{k},\uparrow}$, and $b^\dagger_{\mathbf{k},\mathbf{q}} = a^\dagger_{\mathbf{k}+\mathbf{q}/2,\uparrow} a^\dagger_{-\mathbf{k}+\mathbf{q}/2,\uparrow}$. Here, $\xi(\mathbf{k}) = \epsilon(\mathbf{k}) - \mu$, where $\epsilon(\mathbf{k}) = k^2/(2M)$ is the energy of the fermions and μ is the chemical potential. The attractive interaction can be written in a separable form as $V_p(\mathbf{k},\mathbf{k}') = -4\pi g \Gamma^*(\mathbf{k})\Gamma(\mathbf{k}')$ where $g > 0$, and $\Gamma(\mathbf{k}) = (k k_0)/(k^2 + k_0^2) Y_{1,0}(\hat{\mathbf{k}})$ is a symmetry factor for the $m_\ell = 0$ (p_z) state. In addition, $k_0 \sim R_0^{-1}$ sets the momentum scale, where R_0 is the interaction range in real space. Furthermore, the diluteness condition ($n R_0^3 \ll 1$) requires $(k_0/k_F)^3 \gg 1$, where n is the density of atoms and k_F is the Fermi momentum.

The Gaussian effective action for H is

$$S_{\mathrm{Gauss}} = S_0 + \frac{\beta}{2} \sum_q \bar{\Lambda}^\dagger(q) \mathbf{F}^{-1}(q) \bar{\Lambda}(q), \quad (2)$$

where $q = (\mathbf{q}, v_\ell)$ with bosonic Matsubara frequency

$v_\ell = 2\ell\pi/\beta$. Here, the vector $\bar{\Lambda}^\dagger(q) = [\Lambda^\dagger(q), \Lambda(-q)]$ is the order parameter fluctuation field, and the matrix $\mathbf{F}^{-1}(q)$ is the inverse fluctuation propagator. The saddle point action is $S_0 = \beta|\Delta_0|^2/(8\pi g) + \sum_p[\beta\xi(\mathbf{k})/2 - \mathrm{Tr}\ln(\beta\mathbf{G}_0^{-1}/2)]$, where $\beta = 1/T$ and the inverse Nambu propagator is $\mathbf{G}_0^{-1} = iw_\ell\sigma_0 - \xi(\mathbf{k})\sigma_3 + \Delta_0^*\Gamma(\mathbf{k})\sigma_- + \Gamma^*(\mathbf{k})\Delta_0\sigma_+$. The fluctuation term in the action leads to a correction to the thermodynamic potential, which can be written as $\Omega_{\mathrm{Gauss}} = \Omega_0 + \Omega_{\mathrm{fluct}}$ with $\Omega_0 = S_0/\beta$ and $\Omega_{\mathrm{fluct}} = \beta^{-1}\sum_q \ln\det[\mathbf{F}^{-1}(q)/(2\beta)]$.

The saddle point condition $\delta S_0/\delta\Delta_0^* = 0$ leads to an equation for the order parameter

$$\frac{1}{4\pi g} = \sum_{\mathbf{k}} \frac{|\Gamma(\mathbf{k})|^2}{2E(\mathbf{k})} \tanh\frac{\beta E(\mathbf{k})}{2}, \tag{3}$$

where $E(\mathbf{k}) = [\xi^2(\mathbf{k}) + |\Delta(\mathbf{k})|^2]^{1/2}$ is the quasiparticle energy, and $\Delta(\mathbf{k}) = \Delta_0\Gamma(\mathbf{k})$ is the order parameter. For the p-wave channel, the scattering amplitude [9] $f(k) = k^2/(-1/a_p + r_pk^2 - ik^3)$ depends on two parameters (a_p is the scattering volume, and r_p has dimensions of inverse length), instead of only one parameter as in the s-wave case [13]. Using $f(k)$, we can eliminate g in favor of a_p via the relation

$$\frac{1}{4\pi g} = -\frac{MV}{16\pi^2 a_p k_0^2} + \sum_{\mathbf{k}} \frac{|\Gamma(\mathbf{k})|^2}{2\epsilon(\mathbf{k})}, \tag{4}$$

where V is the volume. Thus, all superfluid properties depend on a_p and r_p (or k_0) as discussed next.

The order parameter equation has to be solved self-consistently with the number equation $N = -\partial\Omega/\partial\mu$ which leads to two contributions $N = N_0 + N_{\mathrm{fluct}}$. $N_0 = -\partial\Omega_0/\partial\mu$ is the saddle point number equation given by

$$N_0 = \sum_{\mathbf{k}} n_0(\mathbf{k}); \qquad n_0(\mathbf{k}) = \frac{1}{2} - \frac{\xi(\mathbf{k})}{2E(\mathbf{k})} \tanh\frac{\beta E(\mathbf{k})}{2}, \tag{5}$$

where $n_0(\mathbf{k})$ is the momentum distribution. Similarly, $N_{\mathrm{fluct}} = -\partial\Omega_{\mathrm{fluct}}/\partial\mu$ is the fluctuation contribution to N given by $N_{\mathrm{fluct}} = -\beta^{-1}\sum_q\{\partial[\det\mathbf{F}^{-1}(q)]/\partial\mu\}/\det\mathbf{F}^{-1}(q)$.

For $T \approx 0$, N_{fluct} is small ($\propto T^4$) compared to N_0 [13] for any interaction strength leading to $N \approx N_0$. In Fig. 1(a), we plot $\Delta_r = \Delta_0/\epsilon_F$ and $\mu_r = \mu/\epsilon_F$ at $T = 0$ as a function of $1/(k_F^3 a_p)$, where $\epsilon_F = k_F^2/(2M)$ is the Fermi energy. Here, we choose $k_0 \approx 200k_F$. Notice that the BCS to BEC evolution range in $1/(k_F^3 a_p)$ is $\sim k_0/k_F$. The weak coupling $\mu = \epsilon_F$ changes continuously to the strong coupling $\mu = -1/(Mk_0 a_p)$ when $k_0^3 a_p \gg 1$. In strong coupling, a_p has to be larger than $a_p > 2/k_0^3$ for the order parameter equation to have a solution with $\mu < 0$, which reflects the Pauli exclusion principle. In addition, the weak coupling $\Delta_0 = 24(k_0/k_F)\epsilon_F\exp[-8/3 + \pi k_0/(4k_F) - \pi/(2k_F^3|a_p|)]$ evolves continuously to a constant $\Delta_0 = 8\epsilon_F[\epsilon_0/(9\epsilon_F)]^{1/4}$ in strong coupling, where $\epsilon_0 = k_0^2/(2M)$. The evolution of Δ_0 and μ are qualitatively similar to recent $T = 0$ results for THS fermion [9] and SHS fermion-boson [8] models. Because of the angular dependence of $\Delta(\mathbf{k})$, the quasiparticle spectrum $E(\mathbf{k})$ is gapless [$\min E(\mathbf{k}) = 0$] for $\mu > 0$, and fully gapped [$\min E(\mathbf{k}) = |\mu|$] for $\mu < 0$. Furthermore, both Δ_0 and μ are nonanalytic exactly when μ crosses the bottom of the fermion energy band $\mu = 0$ at $1/(k_F^3 a_p) \approx 0.5$. The nonanalyticity does not occur in the first derivative of Δ_0 or μ as it is the case in two dimensions [10], but occurs in the second and higher derivatives. Therefore, the evolution from BCS to BEC is not a crossover as in the s-wave case [13]; instead a topological gapless to gapped quantum phase transition [7,10] occurs when $\mu = 0$.

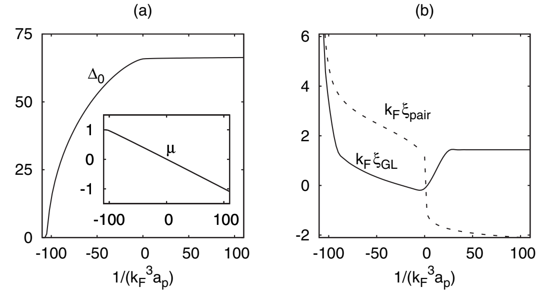

FIG. 1. Plots of reduced (a) order parameter amplitude $\Delta_r = \Delta_0/\epsilon_F$ and chemical potential $\mu_r = \mu/\epsilon_F$, and (b) average Cooper pair size $k_F\xi_{\mathrm{pair}}$ at $T = 0$ and GL coherence length $k_F\xi_{\mathrm{GL}}^{zz}$ at $T = T_c$ in a logarithmic scale versus $1/(k_F^3 a_p)$.

In Fig. 2, we show the momentum distribution $n_0(k_x = 0, k_y, k_z)$ in the BCS side ($\mu > 0$) for $1/k_F^3 a_p = -1$ and in the BEC side ($\mu < 0$) for $1/k_F^3 a_p = 1$. When $k_z/k_F = 0$, $n_0(k_x = 0, k_y, k_z)$ is largest in the BCS side, but it vanishes along $k_z/k_F = 0$ in the BEC side. As the interaction increases the Fermi sea with locus $\xi(\mathbf{k}) = 0$ is suppressed, and pairs of atoms with opposite momenta become more tightly bound. As a result, the large momentum distribution in the vicinity of $\mathbf{k} = \mathbf{0}$ splits into two peaks around finite $\mathbf{k}$, reflecting the p-wave symmetry of these tightly bound states. Thus, $n_0(\mathbf{k})$ for the p-wave case has a major re-

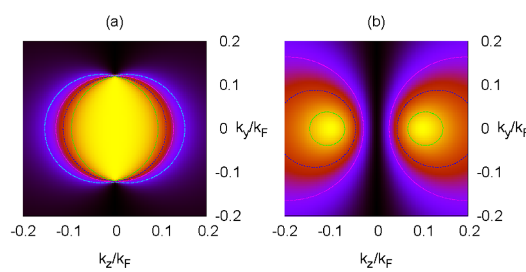

FIG. 2 (color online). Contour plots of momentum distribution $n_0(k_x = 0, k_y, k_z)$ in (a) BCS side ($\mu > 0$) for $1/(k_F^3 a_p) = -1$ and (b) BEC side ($\mu < 0$) for $1/(k_F^3 a_p) = 1$ versus momentum k_y/k_F and k_z/k_F.

arrangement in $\mathbf{k}$ space with increasing interaction, in sharp contrast to the s-wave case, where $n_0(\mathbf{k})$ broadens without qualitative changes [13]. This qualitative difference between p-wave and s-wave symmetries around $\mathbf{k} = \mathbf{0}$ explicitly shows a direct measurable consequence of the gapless to gapped quantum phase transition when $\mu = 0$, since $n_0(\mathbf{k})$ depends explicitly on $E(\mathbf{k})$. Notice that $n_0(k_x, k_y, k_z = 0) = \{1 - \mathrm{sgn}[\xi(\mathbf{k})]\}/2$ for any μ, and that $n_0(k_x, k_y = 0, k_z)$ is trivially obtained from $n_0(k_x = 0, k_y, k_z)$, since $n_0(\mathbf{k})$ is symmetric in k_x, k_y.

Next we discuss p-wave superfluidity near T_c. For $T = T_c$ ($\Delta_0 = 0$), $N_0 = \sum_{\mathbf{k}} n_F[\xi(\mathbf{k})]$ corresponds to the number of unbound fermions. Here, $n_F(w) = 1/[\exp(\beta w) + 1]$ is the Fermi distribution. The fluctuation contribution $N_{\rm fluct}$ is obtained as follows. The matrix $\mathbf{F}^{-1}(q)$ can be simplified to yield

$$L^{-1}(q) = \frac{1}{4\pi g} - \sum_{\mathbf{k}} \frac{1 - n_F(\xi_+) - n_F(\xi_-)}{\xi_+ + \xi_- - i v_\ell} |\Gamma(\mathbf{k})|^2, \quad (6)$$

which is the generalization of the s-wave case [13]. Here, $L^{-1}(q) = \mathbf{F}_{11}^{-1}(q)$, and $\xi_\pm = \xi(\mathbf{k} \pm \mathbf{q}/2)$. The resulting action then leads to the thermodynamic potential $\Omega_{\rm Gauss} = \Omega_0 + \Omega_{\rm fluct}$, where $\Omega_{\rm fluct} = -\beta^{-1}\sum_q \ln[\beta L(q)]$.

The branch cut (scattering) contribution $\Omega_{\rm sc}$ to $\Omega_{\rm fluct}$ is obtained by writing $\beta L(q)$ in terms of the phase shift $\delta(\mathbf{q}, w) = \arg[\beta L(\mathbf{q}, w + i0^+)]$, leading to $\Omega_{\rm sc} = -\pi^{-1}\sum_{\mathbf{q}} \int_{w_q^*}^{\infty} n_B(w)\tilde{\delta}(\mathbf{q}, w) dw$, where $w_{\mathbf{q}}^* = |\mathbf{q}|^2/(4M) - 2\mu$ and $\tilde{\delta}(\mathbf{q}, w) = \delta(\mathbf{q}, w) - \delta(\mathbf{q}, 0)$. Here, $n_B(w) = 1/[\exp(\beta w) - 1]$ is the Bose distribution. For each $\mathbf{q}$, the integral contributes only for $w > w_{\mathbf{q}}^*$, since $\delta(\mathbf{q}, w) = 0$ otherwise. Thus, the branch cut contribution to the number equation $N_{\rm sc} = -\partial \Omega_{\rm sc}/\partial \mu$ is given by

$$N_{\rm sc} = \frac{1}{\pi} \sum_{\mathbf{q}} \int_0^\infty \left[\frac{\partial n_B(\tilde{w})}{\partial \mu} + n_B(\tilde{w}) \frac{\partial}{\partial \mu} \right] \tilde{\delta}(\mathbf{q}, \tilde{w}) dw, \quad (7)$$

where $\tilde{w} = w + w_{\mathbf{q}}^*$.

When $a_p < 0$, there are no bound states above T_c and $N_{\rm sc}$ represents the correction due to scattering states. On the other hand, when $a_p > 0$, there may also be bound states in the two-fermion spectrum, represented by poles with $w < w_{\mathbf{q}}^*$. For arbitrary $1/(k_F^3 a_p)$, the evaluation of the pole (bound state) contribution $N_{\rm bs}$ requires heavy numerics. However, in strong coupling,

$$N_{\rm bs} = 2 \sum_{\mathbf{q}} n_B[w_{\mathbf{q}} - \mu_B], \quad (8)$$

where $w_{\mathbf{q}} = |\mathbf{q}|^2/(4M)$ and $\mu_B = -E_b + 2\mu$. Here, we use $1/(4\pi g) = \sum_{\mathbf{k}} |\Gamma(\mathbf{k})|^2/[2\epsilon(\mathbf{k}) - E_b]$ to express Eq. (8) in terms of binding energy $E_b < 0$. Notice that the expression for $N_{\rm bs}$ given above is good only for couplings where $\mu_B < 0$. Thus, our results for $k_0 \approx 200 k_F$ are not strictly valid when $0 < 1/(k_F^3 a_p) < 1/(k_F^3 a_p^*) \sim 5$, where a_p^* corresponds to $\mu_B = 0$. Therefore, in this region we interpolate. The binding energy in the BEC regime is $E_b = -2/(M k_0 a_p)$ (when $k_0^3 a_p \gg 1$). This result is consistent with a T-matrix calculation [9], where $E_b = 1/(M a_p r_p)$ with $r_p = -2/(k_0^2 a_p) - \pi k_0^2/(4M^2 V) \sum_{\mathbf{k}} |\Gamma(\mathbf{k})|^2/\epsilon^2(\mathbf{k})$. This leads to $r_p = -k_0/2$ (when $k_0^3 a_p \gg 1$), indicating that both approaches produce the same result.

To obtain the evolution from BCS to BEC, we solve numerically the number $N = N_0 + N_{\rm sc} + N_{\rm bs}$ and order parameter equations. In Fig. 3(a), we plot $T_r = T_c/\epsilon_F$ and $\mu_r = \mu/\epsilon_F$ as a function of $1/(k_F^3 a_p)$. The weak coupling $T_c = (8/\pi)\epsilon_F \exp[\gamma - 8/3 + \pi k_0/(4k_F) - \pi/(2k_F^3 |a_p|)]$ evolves continuously to the dilute Bose gas $T_c = 2\pi[2n_B/\zeta(3/2)]^{2/3}/M_B = 0.137\epsilon_F$ in the BEC regime, where $\gamma \approx 0.577$ is the Euler's constant and $n_B = n/2 = k_F^3/(12\pi^2)$ is the density and $M_B = 2M$ is the mass of the bosons. However, the saddle point $T_0 \approx E_b/[2\ln(E_b/\epsilon_F)^{3/2}]$ increases with $1/(k_F^3 a_p)$, and is a measure of the pair dissociation temperature [13]. Notice that the ratio of $\tilde{\Delta}(k_F)/T_c = \Delta_0 \Gamma_k(k_F)/T_c$ in the BCS limit is $3\pi/e^\gamma$. The hump in the intermediate regime is similar to the one observed in a fermion-boson model [12]. Furthermore, similar humps were also calculated in the s-wave case [13]; however, a fully self-consistent numerical approach may be required to determine whether these humps are physical.

The weak coupling $\mu = \epsilon_F$ evolves continuously to the strong coupling $\mu = -1/(M k_0 a_p)$ (when $k_0^3 a_p \gg 1$) leading to $\mu = E_b/2$. Notice that μ crosses the bottom of the band at $1/(k_F^3 a_p) \approx 0.5$, i.e., after the two-body bound state threshold $1/(k_F^3 a_p) = 0$ is reached. The evolution of μ at $T = 0$ (Fig. 1) and $T = T_c$ (Fig. 3) is similar, but very different from the s-wave case [13]. However, another result for μ versus $1/(k_F^3 a_p)$ at $T = T_c$ (much like the s-wave case) was obtained in Ref. [12] using a fermion-boson model. In Fig. 3(b), we also plot the fractions of unbound ($F_0 = N_0/N$), scattering ($F_{\rm sc} = N_{\rm sc}/N$), and bound ($F_{\rm bs} = N_{\rm bs}/N$) fermions as a function of $1/(k_F^3 a_p)$.

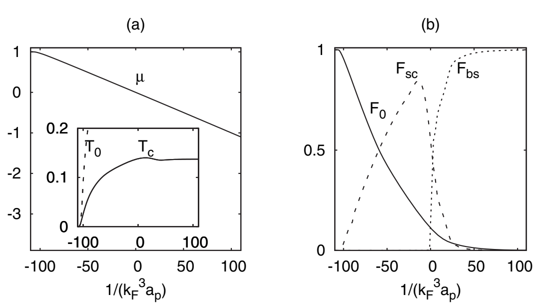

FIG. 3. Plots of reduced (a) critical temperature $T_r = T_c/\epsilon_F$ and chemical potential $\mu_r = \mu/\epsilon_F$ (inset), and (b) fraction of unbound $F_0 = N_0/N$, scattering $F_{\rm sc} = N_{\rm sc}/N$, and bound $F_{\rm bs} = N_{\rm bs}/N$ fermions at $T = T_c$ versus $1/(k_F^3 a_p)$.

While N_0 (N_{bs}) dominates in weak (strong) coupling, N_{sc} is dominant at the intermediate regime.

Next, for the SHS with p_z symmetry near T_c, we obtain the TDGL equation [13]

$$\left[a + b|\Lambda(x)|^2 - \sum_{i,j} \frac{c_{ij}}{2M} \nabla_i \nabla_j - id\frac{\partial}{\partial t}\right]\Lambda(x) = 0 \quad (9)$$

in the real space $x = (\mathbf{x}, t)$ representation. For general p-wave THS states, additional gradient terms may exist [14]. The time-independent expansion coefficients are given by $a = 1/(4\pi g) - \sum_{\mathbf{k}} X|\Gamma(\mathbf{k})|^2/[2\xi(\mathbf{k})]$, and $c_{ij} = \sum_{\mathbf{k}}\{X\delta_{ij}/[8\xi^2(\mathbf{k})] - \beta Y\delta_{ij}/[16\xi(\mathbf{k})] + \beta^2 XYk_ik_j/[16M\xi(\mathbf{k})]\}|\Gamma(\mathbf{k})|^2$, where δ_{ij} is the Kronecker delta, $X = \tanh[\beta\xi(\mathbf{k})/2]$, and $Y = \mathrm{sech}^2[\beta\xi(\mathbf{k})/2]$. Notice that c_{ij} is a tensor due to the anisotropy of the order parameter, which is in sharp contrast to the s-wave case [13]. The coefficient of the nonlinear term is $b = \sum_{\mathbf{k}}\{X/[4\xi^3(\mathbf{k})] - \beta Y/[8\xi^2(\mathbf{k})]\}|\Gamma(\mathbf{k})|^4$. The time-dependent coefficient has real and imaginary parts and is given by $d = \sum_{\mathbf{k}} X|\Gamma(\mathbf{k})|^2/[4\xi^2(\mathbf{k})] + i\beta N(\epsilon_F)\mu^{3/2}\Theta(\mu)/(32\epsilon_0\epsilon_F^{1/2})$, where $\Theta(\mu)$ is the Heaviside function. As the coupling grows, the coefficient of the propagating term (Re[d]) increases, while the damping term (Im[d]) decreases until it vanishes for $\mu \leq 0$, indicating an undamped dynamics for $\Lambda(x)$.

In weak coupling ($\mu = \epsilon_F$), we find $a = \kappa_w \ln(T/T_c)$, $b = 2\kappa_w\epsilon_F\zeta(3)/(5\pi T_c^2\epsilon_0)$, $c_{xx} = c_{yy} = c_{zz}/3 = 7\kappa_w\epsilon_F\zeta(3)/(20\pi^2T_c^2)$, $c_{i\neq j} = 0$, and $d = \kappa_w[1/(4\epsilon_F) + i\pi/(8T_c)]$, where $\kappa_w = \epsilon_F N(\epsilon_F)/(4\pi\epsilon_0)$ and $\zeta(x)$ is the zeta function. By rescaling the order parameter $\Psi_w(x) = \sqrt{b/\kappa_w}\Lambda(x)$, one obtains the anisotropic TDGL equation $-\epsilon\Psi_w + |\Psi_w|^2\Psi_w - \sum_i(\xi_{GL}^{ii})^2\nabla_i^2\Psi_w + \tau_{GL}\partial_t\Psi_w = 0$ with characteristic lengths $\xi_{ii}^2 = c_{ii}/(2Ma) = (\xi_{GL}^{ii})^2/\epsilon$ and time $\tau = -id/a = \tau_{GL}/\epsilon$ scale. Here, $\epsilon = (T_c - T)/T_c$ with $|\epsilon| \ll 1$, $k_F\xi_{GL}^{xx} = k_F\xi_{GL}^{yy} = k_F\xi_{GL}^{zz}/3 = \sqrt{7\zeta(3)/(20\pi^2)}(\epsilon_F/T_c)$, and $\tau_{GL} = -i/(4\epsilon_F) + \pi/(8T_c)$ are typical BCS results [14]. The system is overdamped since $T_c \ll \epsilon_F$ reflecting the presence of two-fermion continuum states into which Cooper pairs can decay.

In strong coupling ($\epsilon_0 \gg |\mu| \gg T_c$), we find $a = \kappa_s(2|\mu| - |E_b|)/8$, $b = 9\kappa_s/(256\pi\epsilon_0)$, $c_{ij} = \kappa_s\delta_{ij}/16$, and $d = \kappa_s/8$, where $\kappa_s = N(\epsilon_F)/(4\sqrt{\epsilon_F\epsilon_0})$. By rescaling the order parameter $\Psi_s(x) = \sqrt{d}\Lambda(x)$, one obtains the conventional Gross-Pitaevskii equation for a dilute gas of bosons $\mu_B\Psi_s + U_B|\Psi_s|^2\Psi_s - \nabla^2\Psi_s/(2M_B) - i\partial_t\Psi_s = 0$ with bosonic chemical potential $\mu_B = -a/d = 2\mu - E_b$, mass $M_B = Md/c_{ii} = 2M$, and repulsive interactions $U_B = b/d^2 = 18\pi/(Mk_0)$. In this regime, $k_F\xi_{GL}^{ii} = [\pi k_0/(36k_F)]^{1/2}$ is independent of a_p and is infinitely large when $k_0/k_F \to \infty$.

The evolution of ξ_{GL}^{ii} follows from $(\xi_{GL}^{ii})^2 = c_{ii}/[2MT_c(\partial a/\partial T)]$, where $\partial a/\partial T = \sum_{\mathbf{k}}(Y/(4T^2) + (\partial\mu/\partial T)\{Y/[4T\xi(\mathbf{k})] - X/[2\xi^2(\mathbf{k})]\})|\Gamma(\mathbf{k})|^2$. Notice that $\partial\mu/\partial T$ vanishes in weak coupling, while it plays an important role in strong coupling. The evaluation of $\partial\mu/\partial T$ for intermediate coupling is very difficult, thus an interpolation for ξ_{GL}^{zz} connecting the weak and strong coupling regimes is shown in Fig. 1(b). While ξ_{GL}^{ii} representing the phase coherence length is large compared to interparticle spacing in both BCS and BEC limits, it has a minimum in the unitarity region $1/(k_F^3a_p) \approx 0$. In contrast, the average Cooper pair size $\xi_{pair}^2 = -\langle\psi(\mathbf{k})|\nabla_{\mathbf{k}}^2|\psi(\mathbf{k})\rangle/\langle\psi(\mathbf{k})|\psi(\mathbf{k})\rangle$, is a decreasing function of interaction, where $\psi(\mathbf{k}) = \Delta(\mathbf{k})/[2E(\mathbf{k})]$ is the $T = 0$ pair wave function. The limiting value of ξ_{pair} in strong coupling is controlled by k_F/k_0. Furthermore, ξ_{pair} is nonanalytic when $\mu = 0$, which is associated with the change in $E(\mathbf{k})$ from gapless (with line nodes) in the BCS to fully gapped in the BEC side.

In summary, we presented a zero and finite temperature analysis of a single-hyperfine state p-wave Fermi gas in 3D within a fermion-only description, where molecules naturally appear as bound states of two-fermions. Our main conclusions are as follows. First, the BCS to BEC evolution in p-wave systems requires another length scale in addition to the scattering volume, while in s-wave systems just the scattering length is sufficient. Second, a quantum phase transition occurs as a function of scattering volume, in contrast with the s-wave case, where the BCS to BEC evolution is a crossover. Third, the p-wave Ginzburg-Landau theory contains anisotropic coherence lengths becoming isotropic only in the BEC limit, in sharp contrast to the s-wave case, where the coherence length is isotropic for all couplings.

We thank NSF (DMR-0304380) for support.

[1] C. A. Regal *et al.*, Phys. Rev. Lett. **90**, 053201 (2003).
[2] C. Ticknor *et al.*, Phys. Rev. A **69**, 042712 (2004).
[3] J. Zhang *et al.*, Phys. Rev. A **70**, 030702 (2004).
[4] C. H. Schunck *et al.*, Phys. Rev. A **71**, 045601 (2005).
[5] K. Günter *et al.*, Phys. Rev. Lett. **95**, 230401 (2005).
[6] J. L. Bohn, Phys. Rev. A **61**, 053409 (2000).
[7] V. Gurarie *et al.*, Phys. Rev. Lett. **94**, 230403 (2005).
[8] C.-H. Cheng and S.-K. Yip, Phys. Rev. Lett. **95**, 070404 (2005).
[9] T.-L. Ho and R. B. Diener, Phys. Rev. Lett. **94**, 090402 (2005).
[10] S. S. Botelho and C. A. R. Sá de Melo, J. Low Temp. Phys. **140**, 409 (2005).
[11] M. Iskin and C. A. R. Sá de Melo, Phys. Rev. B **72**, 224513 (2005).
[12] Y. Ohashi, Phys. Rev. Lett. **94**, 050403 (2005).
[13] C. A. R. Sá de Melo *et al.*, Phys. Rev. Lett. **71**, 3283 (1993).
[14] A. J. Leggett, Rev. Mod. Phys. **47**, 331 (1975).